

Conference materials

UDC 538.956

DOI: <https://doi.org/10.18721/JPM.161.104>

Complex permittivity of graphene-containing shungite within 0.05–15 MHz

R.I. Korolev ¹✉, I.V. Antonets ¹, E.A. Golubev ²

¹ Department of Radiophysics, Pitirim Sorokin Syktyvkar State University, Syktyvkar, Russia;

² Institute of Geology of Komi SC, RAS, Syktyvkar, Russia

✉ korolev36a@gmail.com

Abstract. The paper presents the results of experimental studies of changes in the complex permittivity of natural graphene-containing shungites with different carbon content. A technique for determining the real and imaginary parts of the permittivity for conducting samples is presented. The dependences of the dielectric loss tangent and the real part of the permittivity on the carbon concentration for three resonant frequencies in the range of 0.05–15 MHz are studied.

Keywords: shungite, permittivity, carbon concentration

Funding: This study was funded by RSF, according to the research project No. 21 47 00019.

Citation: Korolev R.I., Antonets I.V., Golubev E.A. Complex permittivity of graphene containing shungite within 0.05–15 MHz, St. Petersburg State Polytechnical University Journal. Physics and Mathematics. 16 (1.1) (2023) 28–32. DOI: <https://doi.org/10.18721/JPM.161.104>

This is an open access article under the CC BY-NC 4.0 license (<https://creativecommons.org/licenses/by-nc/4.0/>)

Материалы конференции

УДК 538.956

DOI: <https://doi.org/10.18721/JPM.161.104>

Комплексная диэлектрическая проницаемость графенсодержащего шунгита в диапазоне 0,05–15 МГц

Р.И. Королев ¹✉, И.В. Антонец ¹, Е.А. Голубев ²

¹ Кафедра радиофизики и электроники, Сыктывкарский государственный университет имени Питирима Сорокина, г. Сыктывкар, Россия;

² Институт геологии Коми НЦ УрО РАН, г. Сыктывкар, Россия

✉ korolev36a@gmail.com

Аннотация. В работе представлены результаты экспериментальных исследований изменения комплексной диэлектрической проницаемости в природных графенсодержащих шунгитах с различным содержанием углерода. Представлена методика определения действительной и мнимой частей диэлектрической проницаемости проводящих образцов. Исследованы зависимости тангенса угла диэлектрических потерь и действительной части диэлектрической проницаемости от концентрации углерода для трех резонансных частот в диапазоне 0,05–15 МГц.

Ключевые слова: шунгит, диэлектрическая проницаемость, концентрация углерода

Финансирование: Исследование выполнено при финансовой поддержке РФФ, в соответствии с исследовательским проектом № 21-47-00019.

Ссылка при цитировании: Королев Р.И., Антонец И.В., Голубев Е.А. Комплексная диэлектрическая проницаемость графенсодержащего шунгита в диапазоне 0,05–15 МГц // Научно-технические ведомости СПбГПУ. Физико-математические науки. 2023. Т. 16. № 1.1. С. 28–32. DOI: <https://doi.org/10.18721/JPM.161.104>

Статья открытого доступа, распространяемая по лицензии CC BY-NC 4.0 (<https://creativecommons.org/licenses/by-nc/4.0/>)

Introduction

In modern technologies, materials with improved and new functional properties are used. Obtaining such materials is often costly from an economic point of view. Therefore, the study of natural objects in order to identify such properties has great prospects. Conductive and high frequency properties are among the most demanded. In this regard, the electrically conductive properties (with emphasis on the determination of the complex permittivity) of the unique natural disordered carbon of shungites from Karelia were studied. A technique for measuring the dielectric constant of conducting samples is presented.

Materials and Methods

The parallelepiped samples were made from natural shungite by cutting and subsequently grinding the faces. The sample height was 1.5 mm, and the side length was 6.0 mm. Two opposite surfaces were metallized by magnetron sputtering of a thin layer of gold in vacuum using argon as a working gas. The total impedance and phase shift at frequencies of 0.05–15 MHz were measured using an E7-29 immittance meter. The specific conductivity for calculating the dielectric loss tangent was determined from the reciprocal value of the electrical resistivity measured at the studied current frequency by the two-probe method [1–3]. To obtain resonance characteristics, a parallel oscillatory circuit with replaceable inductors in a shielded case was used, connected to UP-5. The air condenser for the oscillatory circuit was made of FR-4 foil fiberglass by milling square-shaped plates with an area of $37.4 \pm 0.1 \text{ mm}^2$. To arrange the plates at a fixed distance and ensure plane-parallelism, 4 spacers were used at the corners of the fiberglass. The distance between the plates was $1.95 \pm 0.01 \text{ mm}$. The plate leads were located on opposite sides to reduce the effect on the capacitance. To determine the interturn capacitance of the inductor and the screen capacitance, tubular ceramic capacitors with a capacitance of $3.23 \pm 0.05 \text{ pF}$ and $6.25 \pm 0.02 \text{ pF}$ were connected in parallel to the oscillatory circuit with an empty air capacitor. Based on the obtained resonant frequencies, the additional capacitance caused by the interturn capacitance of the coil and the screen capacitance was calculated. The resonant frequencies were determined by the method of approximation of the Lorentz function from the graphic dependences of the impedance on the frequency [3, 4]. The estimate of the accuracy of calculating the permittivity by the method of standard deviations was 16%.

Consider an oscillatory circuit consisting of a coil with inductance L and an interturn capacitance C_L and an air plane-parallel capacitor connected in parallel with a capacitance C_0 . The inductor is placed in a metal shield to reduce the influence of external electromagnetic field. The resonant frequency of an empty circuit is determined by the formula [5]:

$$f_0 = \frac{1}{2\pi [L(C_0 + C_L)]^{1/2}}, \quad (1)$$

where the capacitance of the capacitor is:

$$C_0 = \frac{\varepsilon_0 S_0}{d_0}, \quad (2)$$

S_0 is condenser area, d_0 is distance between plates, ε_0 is vacuum permittivity.

When a sample is introduced into the gap between the capacitor plates, the circuit frequency will change:

$$f_x = \frac{1}{2\pi [L(C_x + C_L)]^{1/2}}, \quad (3)$$

where C_x is capacitance of a capacitor with installed sample.

The location of the sample in the measuring capacitor of the oscillatory circuit is shown in Fig. 1. Due to the complexity of manufacturing the dimensions of the sample equal to the dimensions of the measuring capacitor, as well as the high conductivity of the sample, it becomes

necessary to take into account the capacitance associated with incomplete filling of the area of the sample measuring capacitor lining C_δ :

$$C_\delta = \frac{\varepsilon_0(S_0 - S_1)}{d_0}, \quad (4)$$

and capacitance due to incomplete filling of the capacitor volume:

$$C_{10} = \frac{\varepsilon_0 S_1}{d_0 - d_1}, \quad (5)$$

where S_1 is sample area, d_1 is sample thickness.

The measuring oscillatory circuit can be represented as an equivalent electrical circuit in Fig. 2, and the capacitance of the measuring capacitor C_x is defined as:

$$C_x = \frac{C_1 C_{10}}{C_1 + C_{10}} + C_\delta, \quad (6)$$

where C_1 is capacitance of the capacitor, formed by the sample:

$$C_1 = \frac{\varepsilon \varepsilon_0 S_1}{d_1}. \quad (7)$$

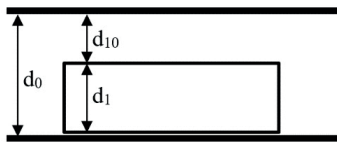


Fig. 1. Cross section of measuring capacitor with sample

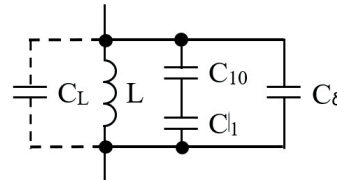


Fig. 2. Equivalent electrical circuit of a parallel oscillatory circuit with a sample

We introduce the following notation:

$$\Delta F = \frac{f_0}{f_x}, \quad (8)$$

$$A = \Delta F^2 - 1 \quad (9)$$

$$B = S_0 A + S_1 \quad (10)$$

Solving Equations (1) and (3) together, taking into account (8–10), we obtain an expression for the real part of the permittivity ε' [5–7]:

$$\varepsilon' = \frac{\varepsilon_0 B + d_0 C_L A}{\varepsilon_0 (S_0 d_0 A - d_1 B) + d_0 C_L A (d_0 - d_1)} d_1, \quad (11)$$

To determine the interturn capacitance we jointly solve Equations (1, 2, 8) with respect to C_L , we obtain:

$$C_L = \frac{-\Delta F^2 C_1 + C_2}{\Delta F^2 - 1}, \quad (12)$$

In this case, C_1 and C_2 are the capacitances of additional capacitors, connected to an unfilled measuring capacitor, ΔF is the ratio of the resonant frequencies of the circuit with these additional capacitances. The dielectric loss tangent is determined by the formula:

$$\tan \delta = \frac{\sigma}{2\pi f_0 \varepsilon_0 \varepsilon'}, \quad (13)$$



where σ — sample conductivity:

$$\sigma = \frac{1}{\rho} = \frac{d_1}{S_1 Z \cos \varphi}, \quad (14)$$

where Z — sample impedance, φ — angle of phase shift between the current and voltage of the probing signal.

The imaginary part of the permittivity is related to the loss tangent by the expression:

$$\varepsilon'' = \varepsilon' \tan \delta, \quad (15)$$

The desired complex permittivity:

$$\varepsilon = \varepsilon' - i\varepsilon''. \quad (16)$$

Results and Discussion

Figures 3 and 4 show the dependences of the permittivity (Fig. 3) and the dielectric loss tangent (Fig. 4) on the carbon concentration of shungites at three different resonant frequencies of the oscillatory circuit: 2.6, 8.7, and 14.36 MHz. As it can be seen from the figures, at the same carbon content, the permittivity somewhat increases with increasing frequency, and the dielectric loss tangent decreases, which corresponds to the behavior of ionic relaxation at the indicated frequencies.

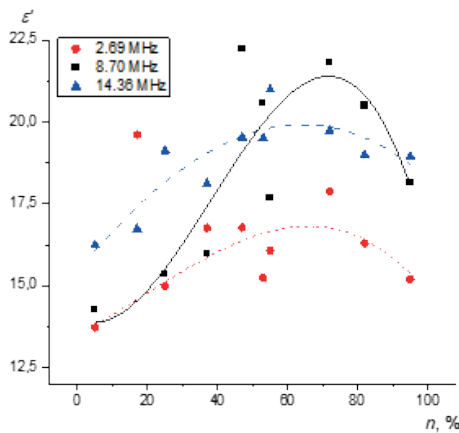


Fig. 3. Dependences of the real part of the permittivity on the carbon concentration at different frequencies

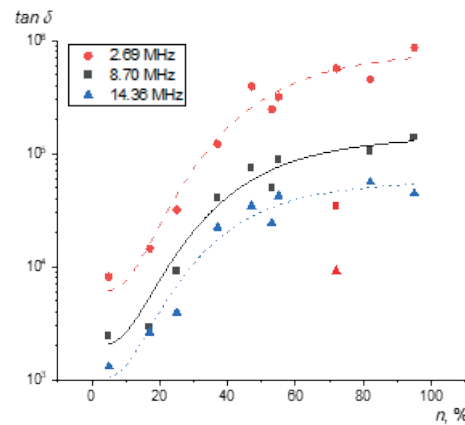


Fig. 4. Dependences of the dielectric loss tangent on the carbon concentration at different frequencies

Shungites have rather high electrical conductivity (hundreds–thousands of S/m) even at low carbon content (from 17% and higher) [1, 2]. Therefore, the dielectric loss tangent of the samples is also very significant, but it decreases with increasing frequency (Fig. 4). Thus, at a carbon concentration of 5%, with an increase in frequency from 2.6 to 8.7 MHz, $\tan \delta$ decreases by a factor of three, and with an increase in frequency from 8.7 to 14.4 MHz, by one and a half times. For high-carbon shungites with a carbon concentration of 90%, with increasing frequency, the dielectric loss tangent decreases by 5 and 2 times, respectively. The qualitative behavior of the dependences of the loss tangent on the carbon concentration is preserved for all frequencies. According to Fig. 4, at a carbon content of 60–70%, the loss tangent begins to saturate and is only weakly dependent on concentration. In this case, due to the smallness of the real part of the permittivity in comparison with the imaginary one, the qualitative behavior ε'' of the carbon content is almost coincident with the dependence of $\tan \delta$.

As can be seen from Fig. 3, the real part of the dielectric constant of shungites varies depending on the frequency in the range of 0.05–15 MHz and the carbon concentration n in the range from 13.5 to 22.5, which corresponds to the values presented in [8]. An increase in the carbon concentration leads to a gradual increase in the real permittivity ε' up to $n = 60$ –70%, at which the dielectric loss tangent saturates. With a further increase in n , the real part of the permittivity sharply decreases. This behavior ε' is associated with an increase in the conductivity of shungite

due to the formation of conductive channels from carbon, which leads to a decrease in the volume of dielectric inclusions and the area of interboundary regions with the dielectric phase. At low carbon content, the main contribution to the dielectric permittivity is made by the ionic and dipole nature of the dielectric permittivity; at high carbon concentrations, the dipole nature begins to transform into atomic one. The peak at the resonant frequency of 8.70 MHz at $n = 70\%$ can be associated with the resonant dispersion of the permittivity, which indicates the ionic nature of the polarization.

Conclusion

In this paper, the dependences of the dielectric loss tangent and the real part of the dielectric constant as a function of carbon concentration for three resonant frequencies in the range of 0.05–15 MHz are studied. The dielectric permittivity in shungite grows with an increase in the carbon content up to $n = 60\text{--}70\%$. In this range of carbon concentration, there is a peak in the dielectric constant. A further sharp decrease in the permittivity with an increase in the carbon content occurs due to an increase in conductivity. The peak at the resonant frequency of 8.70 MHz at $n = 70\%$ indicates the ionic nature of the polarization.

REFERENCES

1. Antonets I.V., Golubev E.A., Shavrov V.G., Shcheglov V.I., Application of the independent channel method for determining the electrical conductivity of graphene-containing shungite, Journal of radio electronics. 7 (2021). <http://jre.cplire.ru/jre/jul21/6/text.pdf>
2. Golubev E.A., Antonets I.V., Shcheglov V.I., Static and dynamic conductivity of nanostructured carbonaceous shungite geomaterials, Materials chemistry and physics. 226 (2019) 195–203.
3. Antonets I.V., Golubev E.A., Korolev R.I., Electrophysical parameters of shungite, AIP Conf. Proc. 2467 (2022) 020026.
4. Antonets I.V., Golubev E.A., Korolev R.I., St. Petersburg Polytechnic University Journal: Physics and Mathematics. (2023) (in press).
5. Keysight, Basics of Measuring the Dielectric Properties of Materials Application Note. (2017).
6. Hewlett-Packard Company, Dielectric constant measurement of solid materials using the 16451B dielectric test fixture Application Note 308–1. (1998).
7. GOST 22372-77 Dielectric materials. Methods of determination of permittivity and powerfactor with in a frequency range of 100 to 5 MHz.
8. Moshnikov I.A., Kovalevsky V.V., Lazareva T.N., Petrov A.V., The use of shungite rocks in the creation of radio shielding composite materials, Petrozavodsk: Geodynamics, magmatism, sedimentogenesis and minerageny of the North-West of Russia. (2007) 272–274.

THE AUTHORS

KOROLEV Roman I.
korolev36a@gmail.com
ORCID: 0000-0002-5091-1385

GOLUBEV Evgeniy A.
yevgenyGolubev74@mail.ru
ORCID: 0000-0001-5354-937X

ANTONETS Igor V.
aiv@mail.ru
ORCID: 0000-0003-1103-4313

Received 29.09.2022. Approved after reviewing 06.12.2022. Accepted 06.12.2022.